

Exploring a glycolytic inhibitor for the treatment of an *FH*-deficient type-2 papillary RCC

Toshinari Yamasaki, Tram Anh T. Tran, Orhan K. Oz, Ganesh V. Raj, Roderich E. Schwarz, Ralph J. DeBerardinis, Xuewu Zhang and James Brugarolas

Background. A 24-year-old woman presented with a 45 cm complex cystic renal mass, which was resected. The tumor was a type-2 papillary renal cell carcinoma (pRCC-2), and several nodules remained. The patient was treated with mammalian target of rapamycin complex 1 (mTORC1) inhibitors, but after 5 months the tumor had progressed. Genetic testing of the patient revealed a novel heterozygous germline mutation in the gene encoding fumarate hydratase (*FH*), an enzyme of the tricarboxylic acid (TCA) cycle. As the tumor exhibited loss of heterozygosity for *FH* and markedly reduced *FH* activity, and in the absence of other established therapies, treatment with the glycolytic inhibitor 2DG (2-deoxy-D-glucose) was explored.

Investigations. CT, histology, immunohistochemistry, genetic studies, 2-deoxy-2-(¹⁸F)fluoro-D-glucose (¹⁸FDG)-PET/CT, *FH* enzymatic assays, reconstitution experiments and *in vitro* studies of the effects of 2DG on *FH*-deficient tumor cells.

Diagnosis. pRCC-2 arising in a patient with a novel germline *FH* mutation and *de novo* hereditary leiomyomatosis and renal cell cancer (HLRCC) syndrome progressing after mTORC1 inhibitor therapy.

Management. Surgical resection of the renal mass, treatment with mTORC1 inhibitors followed by 2DG. Unfortunately, 2DG was not effective, and the patient died several weeks later.

Yamasaki, T. et al. *Nat. Rev. Urol.* advance online publication 8 February 2011; doi:10.1038/nrurol.2010.234

The case

A 24-year-old woman was referred from an outside hospital where she had presented a few days earlier with increasing abdominal discomfort, bloating, anorexia and weight loss. She was found to have a 45 cm complex cystic mass occupying most of her abdomen (Figure 1a) and a hemoglobin level of 7 g/dl. The patient was transferred for definitive treatment. No liver or lung metastases were observed. She underwent arteriography with successful transarterial alcohol embolization of a left anterolateral artery that was presumed to represent the left renal artery. During the procedure, 1.6 l of a dark, rusty fluid with a small amount of fatty-appearing debris was drained, and biopsies were performed. The biopsy material was necrotic, and no definitive pathological diagnosis could be established. Her hemoglobin level stabilized after the procedure. Contrast-enhanced brain MRI showed no evidence of brain metastasis. 4 weeks later, the patient was electively readmitted for surgical resection. The mass was adherent to the mesentery, spleen and pancreas, which necessitated partial colectomy, splenectomy and partial pancreatectomy.

Pathological studies revealed two tumor masses attached to each other measuring 45 cm and 13 cm at their largest diameter. Microscopic analyses showed a

high-grade adenocarcinoma with fibrovascular papillae lined by stratified, large, pleomorphic cells with eosinophilic cytoplasm and large, prominent nucleoli (Figure 2). The tumor invaded into the pancreas and involved multiple lymph nodes, including pericolonic nodes. Immunohistochemical analyses showed the tumor cells to be strongly positive for vimentin, focally positive for CD10, and negative for cytokeratins 7 and 20. Overall, the diagnosis was most consistent with a type-2 papillary renal cell carcinoma (pRCC-2).

The patient recovered well from the surgery, and received meningococcal, pneumococcal and *Haemophilus influenzae* type b vaccines prior to discharge. Approximately 1 month after surgery, CT of the chest, abdomen and pelvis showed several discrete enhancing nodules in the abdomen and paravertebral area that had increased in size and measured up to 3 cm in diameter (Figure 1b). Temsirolimus, an inhibitor of mammalian target of rapamycin complex 1 (mTORC1; also known as mTOR) that has shown unrestricted activity against RCC,¹ was started. Temsirolimus was given at the standard dose of 25 mg intravenously once a week; however, the patient had difficulty attending weekly infusions, and, after two doses, the treatment was switched to daily, oral everolimus 10 mg. Everolimus, like temsirolimus, is approved for renal cancer, and although studied in a different context,² both drugs are sirolimus analogs

Department of Internal Medicine, Hematology–Oncology division (T. Yamasaki, T. A. T. Tran, J. Brugarolas), Department of Radiology (O. K. Oz), Department of Urology (G. V. Raj), Department of Surgery (R. E. Schwarz), Department of Pediatrics (R. J. DeBerardinis), Department of Pharmacology (X. Zhang), University of Texas Southwestern Medical Center, Dallas, TX 75390, USA.

Correspondence to: J. Brugarolas (james.brugarolas@utsouthwestern.edu)

Competing interests

The authors declare no competing interests.

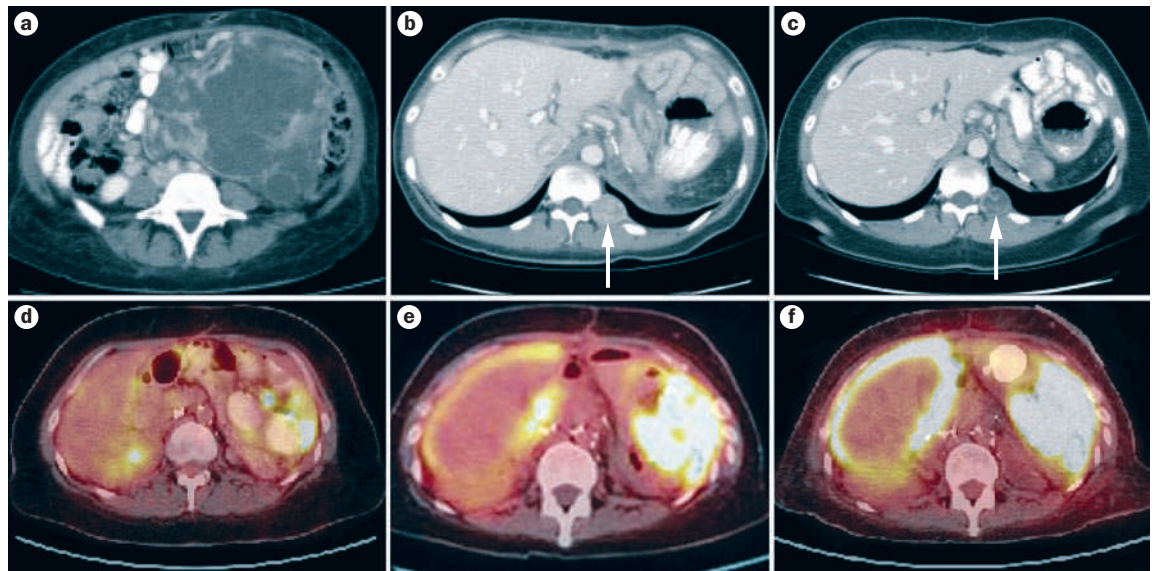


Figure 1 | CT and ¹⁸F-FDG-PET/CT imaging throughout treatment. CT performed **a** | at presentation, **b** | after surgery and **c** | after treatment with mTORC1 inhibitors. Arrows show the largest paraspinous mass. ¹⁸F-FDG-PET/CT performed **d** | before 2DG therapy, **e** | after treatment with once-daily 2DG and **f** | after treatment with 2DG every 8 h or 6 h. Abbreviations: 2DG, 2-deoxy-D-glucose; ¹⁸F-FDG, 2-deoxy-2-(¹⁸F)fluoro-D-glucose; mTORC1, mammalian target of rapamycin complex 1.

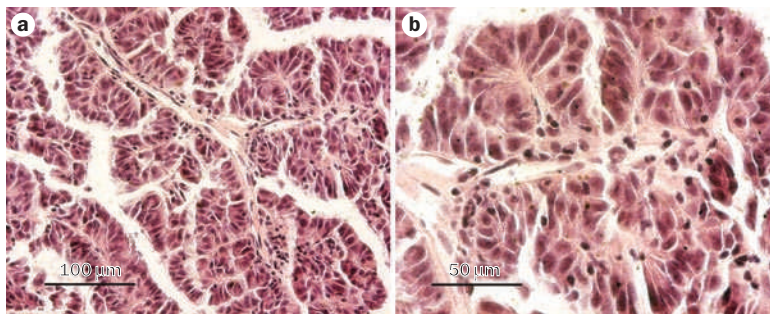


Figure 2 | Representative photomicrographs of tumor sections, showing fibrovascular papillae lined by stratified, large, pleomorphic cells with eosinophilic cytoplasm and large, prominent nucleoli. Hematoxylin and eosin staining, **a** | original magnification $\times 200$, **b** | original magnification $\times 400$.

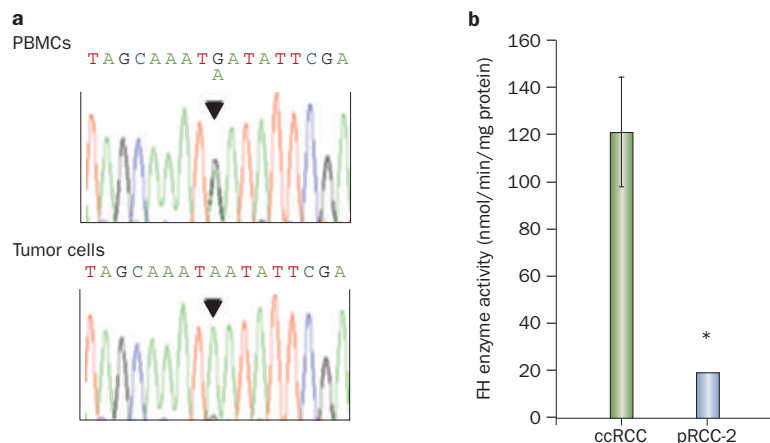


Figure 3 | *FH* gene sequencing and enzymatic activity analyses. **a** | DNA sequence chromatograms from PBMCs and tumor cells. **b** | *FH* enzymatic activity in the pRCC-2 vs a panel of five ccRCCs. Data are means \pm SE. * $P < 0.01$. Abbreviations: ccRCC, clear-cell renal cell carcinoma; *FH*, fumarate hydratase; PBMCs, peripheral blood mononuclear cells; pRCC-2, type-2 papillary renal cell carcinoma.

and are likely to act in the same manner. 3 months later, CT showed a modest reduction in the size of the metastases (Figure 1c). The largest paraspinous mass was treated with additional stereotactic radiation therapy.

The patient had no family history of cancer and both her parents were alive and well, but, given her young age and advanced presentation with an uncommon tumor type, consideration was given to the possibility that a *de novo* germline predisposing mutation had arisen. In particular, given the tumor histology, there was a suspicion of hereditary leiomyomatosis and renal cell cancer (HLRCC). HLRCC is a syndrome with an autosomal dominant pattern of inheritance caused by germline loss-of-function mutations in the gene encoding fumarate hydratase (*FH*).^{3,4} *FH* functions as a classic two-hit tumor suppressor gene,⁵ and the resulting tumors typically exhibit loss of heterozygosity (LOH).⁶ HLRCC is characterized by cutaneous and uterine leiomyomas and highly aggressive renal cell carcinomas (typically type-2 papillary tumors).⁷ Although no cutaneous leiomyomas were observed on skin examination, she was noted to have uterine fibroids. The patient was initially uncertain about genetic testing, but she subsequently agreed. Sequencing analyses of DNA from peripheral blood mononuclear cells showed a heterozygous germline *FH* mutation (c.1021G>A) (Figure 3a). The mutation resulted in a nonconservative substitution of an evolutionarily conserved residue (Asp341Asn). This variant was not known to represent a polymorphism, and was not found among previously reported mutations.⁸

Importantly, sequencing studies of tumor DNA indicated LOH with nearly undetectable amounts of the wild-type *FH* allele (Figure 3a). In addition, enzymatic assays showed, in comparison to a panel of clear-cell RCC (ccRCC) tumors, very low levels of *FH* activity (Figure 3b). *FH* functions as a tetramer,⁹ and studies of

Box 1 | Characterization of the *FH* mutation

To evaluate the effects of $FH^{Asp341Asn}$, we first examined the crystal structure of the *FH* holoenzyme (Protein Data Bank ID 3E04). We found that Asp341, an acidic, negatively charged amino acid, was involved in an intramolecular interaction with Lys337, a basic, positively charged residue, and that this interaction was buried deep within the intermolecular interface (Figure 4a). A substitution of Asp341 for Asn, an uncharged amino acid, would leave Lys337 unpaired, resulting in an energetically unfavorable net positive charge in the hydrophobic intermolecular interface, which would be expected to destabilize the tetramer. To determine experimentally whether $FH^{Asp341Asn}$ would form stable tetrameric complexes, the mutation was engineered by site-directed mutagenesis and introduced into *FH*-deficient UOK262 cells (Figure 4b). In contrast to UOK262 cells in which wild-type *FH* was introduced, tetramers did not form in $FH^{Asp341Asn}$ -reconstituted cells (Figure 4c). These data suggest that $FH^{Asp341Asn}$ does not form homotetramers, and this observation may explain the lack of *FH* activity in the tumor.

Abbreviation: *FH*, fumarate hydratase.

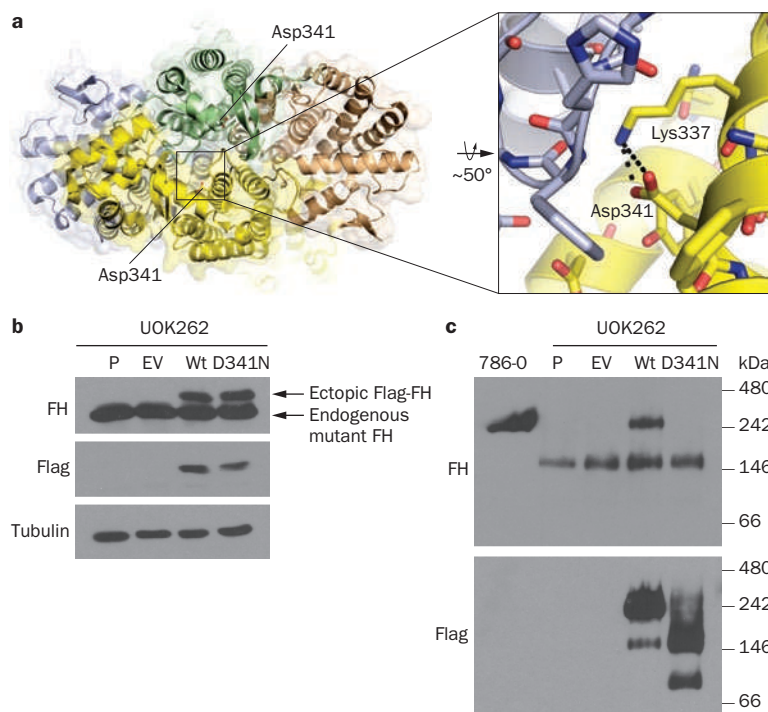


Figure 4 | Characterization of the mutant $FH^{Asp341Asn}$ protein. **a** | Quaternary structure of the human wild-type *FH* tetramer, color-coded to show each subunit, with a depiction of the intramolecular interaction between the negatively charged carboxylic acid group in Asp341 and the positively charged ϵ -amino group of Lys337 (inset). **b** | Western blot of the pRCC-2-derived cell line UOK262 (P, parental cells) transduced with either an empty vector (EV) or vectors driving the expression of Flag-tagged wild-type *FH* (Wt) or $FH^{Asp341Asn}$. The exogenous protein (encoded by the retrovirus) can be distinguished from the endogenous protein by a short amino acid sequence (a tag) that was added to the *FH* sequence. Flag-tagged *FH* protein migrates in gels with a slower mobility and shows on top. The lower band, seen across all the samples and similarly recognized by anti-*FH* antibodies, is endogenous *FH*, which is mutant and nonfunctional in UOK262 cells. The ectopic, retrovirally encoded protein can also be recognized by antibodies directed specifically against the Flag tag (second panel). Tubulin is used as a control to show that the differences in signal are not due to differences in the amount of protein loaded. The blot shows expression in the corresponding lanes of ectopically expressed wild-type and mutant $FH^{Asp341Asn}$ protein. **c** | Western blot of protein extracts of the same cells plus a 786-O clear-cell RCC cell line as a control. In this case, samples were processed and evaluated under nonreducing conditions that allow proteins to remain bound to each other in complexes. This panel shows that, while *FH* protein is found in large complexes (tetramers) in 786-O cells, in UOK262 cells endogenous mutant *FH*, while still able to assemble, forms smaller complexes. The introduction of wild-type *FH* into UOK262 cells restores the formation of normal-sized tetrameric complexes, whereas the introduction of $FH^{Asp341Asn}$ fails to restore normal-sized complexes. Abbreviations: *FH*, fumarate hydratase; p-RCC-2, type-2 papillary renal cell carcinoma.

the previously reported crystal structure and reconstitution experiments suggested that the patient's mutation interfered with oligomerization and that mutant *FH* did not form stable tetramers (Box 1, Figure 4).

FH-deficient cells express high levels of glucose transporters,^{10–12} leading us to hypothesize that 2-deoxy-2-(¹⁸F)fluoro-D-glucose (¹⁸FDG)-PET (which is not recommended for routine RCC evaluation) might be a suitable imaging modality to use in this patient. ¹⁸FDG-PET/CT showed diffuse ¹⁸FDG uptake throughout the abdomen and pelvis, indicative of peritoneal carcinomatosis (Figure 1d). Importantly, the size of tumor implants was such that they would have escaped recognition by CT alone. In addition, a dilated loop of small bowel suggestive of a partial obstruction was noted. Owing to the presence of progressive disease, everolimus treatment was stopped.

There are no established therapies for metastatic *FH*-deficient pRCC-2. While pRCC-2 also occurs sporadically, *FH* has not been found to be mutated in sporadic tumors;^{13,14} indeed, whether sporadic and familial pRCC-2 are related entities remains to be determined. Germline *FH* mutations are uncommon, and there is no established treatment for metastatic pRCC-2 in HLRCC patients.¹⁵ Even for sporadic pRCC-2, which may represent a different clinical entity, the role of other RCC therapies, including small-molecule tyrosine kinase inhibitors like sunitinib (which have been largely evaluated against tumors with a clear-cell component) is questionable. Whereas a retrospective study suggested that sunitinib may be active against non-clear-cell RCC,¹⁶ a small prospective study in patients with papillary RCC showed very disappointing results.¹⁷ In addition, these agents can cause intestinal perforation: although this is a rare occurrence, the risk may be increased in the context of peritoneal carcinomatosis and an impending

partial small bowel obstruction. On this basis, and following a discussion with the patient about the situation, we decided to explore alternative treatment options.

We determined that the glycolytic inhibitor 2-deoxy-D-glucose (2DG) might be beneficial for the patient, on the basis that *FH* deficiency disrupts the tricarboxylic acid (TCA) cycle, resulting in profoundly impaired mitochondrial ATP production and a reliance on glycolysis for energy production.^{12,18,19} There is currently great interest in the development of glycolytic inhibitors, such as 2DG, as cancer treatments.²⁰ 2DG was particularly attractive in the current case because the tumor

Box 2 | Sustained 2DG exposure required to abrogate tumor cell proliferation *in vitro*

Pharmacokinetic studies with a daily 2DG dose similar to that used in our patient had shown a peak blood concentration of 10–12 mg/dl and an elimination half-life of 5–6 h.²¹ Based on these data, we estimated that 2DG levels would be ~10% of fasting circulating glucose levels for ~4 h. We set out to determine the effects of such an exposure on *FH*-deficient tumor cells in culture. UOK262 cells, which do not tolerate low glucose levels, could be cultured on near-physiological glucose concentrations (150 mg/dl). To simulate daily dosing, the medium was supplemented with 10% 2DG for 4 h a day (pulse treatment). While this 2DG regimen decreased cell proliferation (Figure 5a), tumor cells continued to expand even with 2DG concentrations as high as 20% (data not shown). By contrast, sustained, uninterrupted treatment with 10% 2DG suppressed cell proliferation (Figure 5b). These data suggested that greater antitumor activity may be achieved in the patient with more-frequent 2DG dosing.

Abbreviations: FH, fumarate hydratase; 2DG, 2-deoxy-D-glucose.

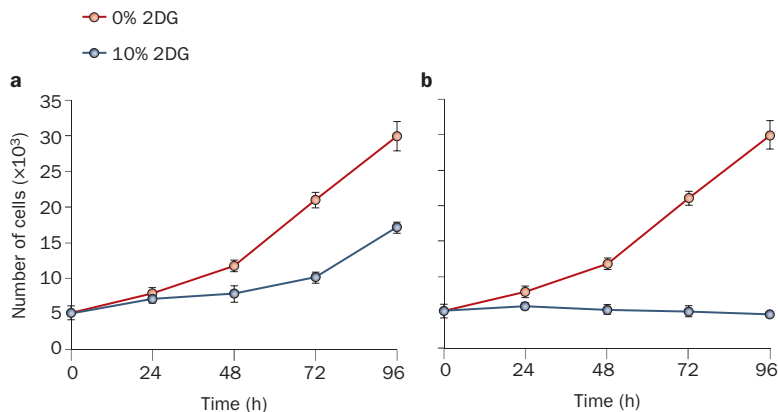


Figure 5 | The effect of 2DG on the proliferation of UOK262 cells. Proliferation curves of UOK262 cells exposed to 0% or 10% 2DG for **a** | 4 h per day (pulse treatment) or **b** | continuously (with daily medium exchanges). Despite pulse 2DG treatment, cell numbers continued to increase. However, proliferation ceased with continuous 2DG treatment. Data are means \pm SE, $n=3$. Abbreviation: 2DG, 2-deoxy-D-glucose.

had shown high avidity for ¹⁸F₂FDG, which, like 2DG, is a glucose analog with a substitution of the hydroxyl group at position 2, suggesting that 2DG would similarly accumulate in tumor cells. 2DG is transported into cells by glucose transporters, and, once inside cells, is phosphorylated by hexokinase to 2DG-6-phosphate. However, in contrast to glucose-6-phosphate, the lack of a hydroxyl group at position 2 precludes further metabolism. Thus, 2DG-6-phosphate acts as a competitive inhibitor of glucose-6-phosphate isomerase, which catalyzes the next step in glycolysis, as well as of glucose-6-phosphate dehydrogenase, which is involved in the pentose phosphate pathway.

Two phase I clinical trials have evaluated 2DG in solid tumors.^{21,22} The studies differed in the maximum tolerated dose, which was reached in one study because of the observation of prolongation of the corrected QT interval (QTc),²¹ but not in the other.²² However, both studies concurred that 2DG was well tolerated.

As there were no clinical trials of 2DG open, and following approval by the institutional review board, a single patient emergent investigational new drug request was filed with the FDA, and the drug was requested

from the investigational new drug holder, Threshold Pharmaceuticals (Redwood City, CA).

Owing to the patient's heterozygous *FH* state, and an expected reduction in *FH* activity, there was a concern that the patient would be at increased risk of 2DG-related toxicities. Furthermore, there have been reports of mutations in patients that not only result in loss-of-function, but that are also dominant-negative and interfere with the function of the wild-type protein encoded by the remaining wild-type allele.²³ While our studies suggested that Asp341Asn interfered with tetramerization, suggesting that it may not act in a dominant-negative fashion, further studies would be required to exclude this possibility. As a precaution, 2DG was started at one-eighth of the target dose of 63 mg/kg. 2DG was administered orally once daily after an overnight fast under direct medical supervision. The patient tolerated the first dose without any problems. Given the advanced nature of her disease and concerns about an impending small bowel obstruction, the 2DG dose was rapidly escalated and, within a period of 8 days, the target dose was reached. The patient's QTc remained within the normal range, and except for grade 1 hypokalemia and hypomagnesemia, no other toxicities were apparent. Unfortunately, however, 1 week after the target dose was reached, the patient developed abdominal pain, nausea and vomiting, and was found to have a complete proximal small bowel obstruction. Exploratory laparotomy revealed diffuse tumor infiltration, but no transition point could be identified. 2DG treatment was stopped, a jejunostomy tube was placed, and the patient was started on total parenteral nutrition (TPN).

2DG did not seem to be effective under the current dosing regimen, and we explored alternative strategies with the use of *in vitro* experiments (Box 2, Figure 5). The results prompted us to attempt more-frequent 2DG administration. Once approval for this regimen had been obtained from the FDA, and while the patient was hospitalized and on telemetry, 2DG (63 mg/kg) was given every 8 h for the first 2 days, followed by every 6 h on subsequent days. To minimize 2DG competition by circulating glucose, carbohydrates were eliminated from the TPN infusion and calories were provided in the form of fat and amino acids. On this regimen, the patient developed symptoms of hypoglycemia, including palpitations, clamminess and transient blurred vision. Circulating glucose levels were within the normal range and ketones were present in the urine. There were no electrolyte abnormalities, arrhythmias or QTc prolongation, and echocardiography showed normal cardiac function. After 4 days on 6-hourly dosing and an interval >24 h off 2DG (to avoid competition with ¹⁸F₂FDG), ¹⁸F₂FDG-PET/CT was performed to evaluate the antitumor activity of the treatment. Compared to a scan performed 3 weeks earlier (Figure 1e), tumor ¹⁸F₂FDG uptake was increased (Figure 1f).

While the increase in ¹⁸F₂FDG uptake may have reflected a compensatory increase in glucose uptake as a result of glycolysis blockade, it could also have indicated tumor progression, and, in the absence of any evidence

of antitumor activity, and despite the short treatment period, further 2DG treatment was stopped. Several weeks later, following a course of sunitinib therapy, the patient developed septic shock, which ultimately led to her death.

Diagnosis

Despite the fact that the *FH* mutation seen in the patient was not previously associated with HLRCC, the diagnosis of HLRCC was supported by other evidence. The mutation was a missense mutation leading to a non-conservative substitution of an amino acid that is conserved throughout evolution and seems to be important for FH tetramerization. In addition, the wild-type allele was lost from the tumor, and the tumor exhibited very low levels of FH enzymatic activity. These data suggest that pRCC-2 probably developed as a result of a pre-disposition conferred by a germline loss-of-function mutation in the *FH* tumor suppressor gene.

Box 3 | 2DG inhibits mTORC1 in *FH*-deficient tumor cells

We studied the effects of 10% 2DG (~1 mM) on extracellular acidification rate (a surrogate for lactic acid production and glycolysis), oxygen consumption rate (an indicator of mitochondrial respiration) and cellular ATP levels in UOK262 cells. Although 2DG blocked glycolysis and lowered ATP levels at 50-fold higher concentrations than those achieved in plasma, at 1 mM (16.4 mg/dl) the effects of 2DG were quite modest (Figure 6a). Even over the course of 24 h, 2DG only moderately affected ATP levels (Figure 6b). However, small changes in the energy state of cells may activate the energy-sensing kinase AMPK, which has been previously linked to mTORC1.^{29,30} Indeed, at pharmacologically relevant concentrations, 2DG led to the activation of AMPK in *FH*-deficient cells (Figure 7). Importantly, AMPK activation was associated with mTORC1 inhibition. To determine whether the inhibition of mTORC1 was mediated by AMPK, we tested whether mTORC1 inhibition by 2DG could be blocked by a drug preventing the activation of AMPK. AMPK inhibition by compound C allowed mTORC1 to remain active despite treatment with 2DG. These data suggest that, at pharmacologically relevant concentrations, 2DG activates AMPK in *FH*-deficient cells and leads to inhibition of mTORC1 in an AMPK-dependent manner.

Abbreviations: 2DG, 2-deoxy-D-glucose; AMPK, AMP-activated protein kinase; FH, fumarate hydratase; mTORC1, mammalian target of rapamycin complex 1.

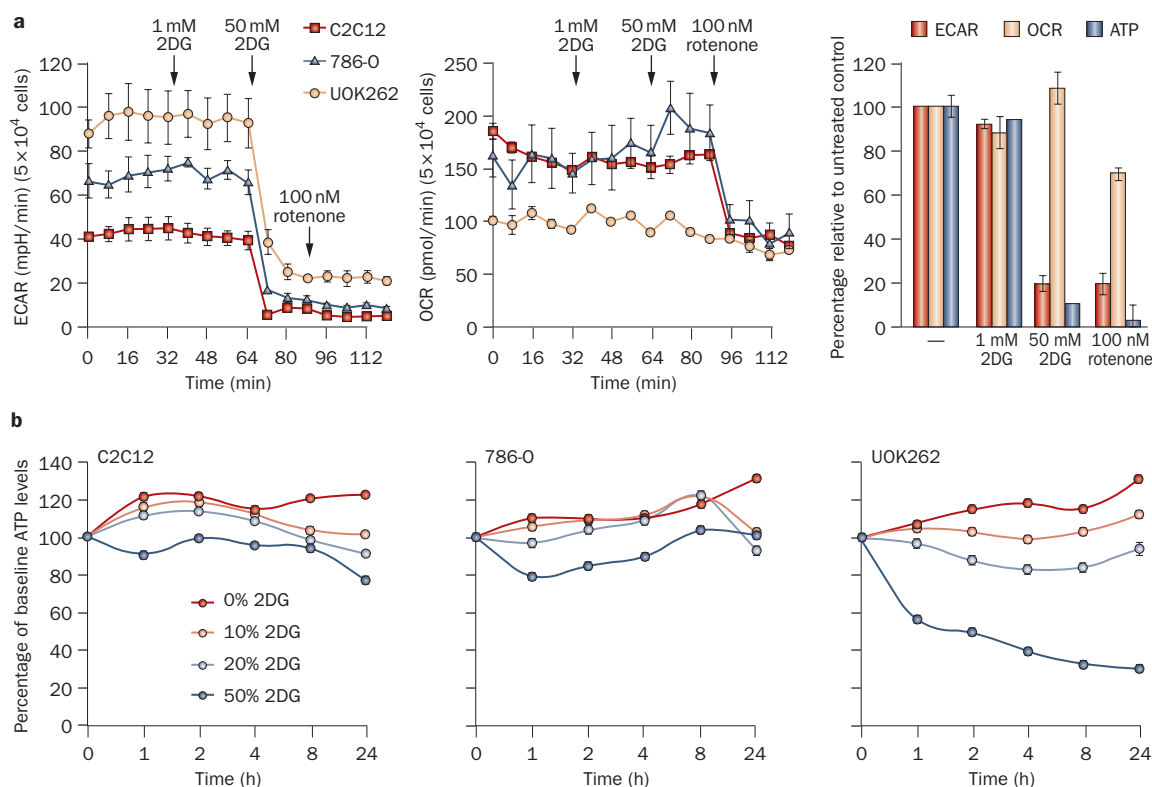


Figure 6 | The effect of 2DG treatment on ECAR, OCR and ATP levels in UOK262 cells and two control cell lines: 786-O and the extensively characterized C2C12 myoblast cell line. **a** | Line graphs show that 1 mM 2DG treatment, equivalent to 16.4 mg/dl (~10%), does not substantially affect lactic acid production or oxygen consumption in any of the cell lines. In contrast, 50-fold higher 2DG concentrations readily block glycolysis and lactic acid production in all cell lines. As expected, treatment with rotenone, a respiratory complex I inhibitor, abrogated oxygen consumption in all the control cells, but did not (also as expected) significantly affect oxygen consumption in *FH*-deficient UOK262 cells, which have a truncated tricarboxylic acid cycle. The bar graph illustrates the effects in UOK262 cells of a 4 h treatment with 1 mM 2DG, followed by a 0.5 h treatment with 50 mM 2DG and, subsequently, a 0.5 h treatment with 100 nM rotenone. **b** | The effects of various 2DG concentrations on ATP levels in the three cell lines over time. The data show a dose-dependent downregulation of ATP levels in UOK262 cells by 2DG. By contrast, control cell lines seem to be less sensitive to 2DG. Note also that 10% 2DG had a very modest effect on total ATP levels in UOK262 cells. Data are means \pm SE, $n=3$. Abbreviations: 2DG, 2-deoxy-D-glucose; ECAR, extracellular acidification rate; OCR, oxygen consumption rate.

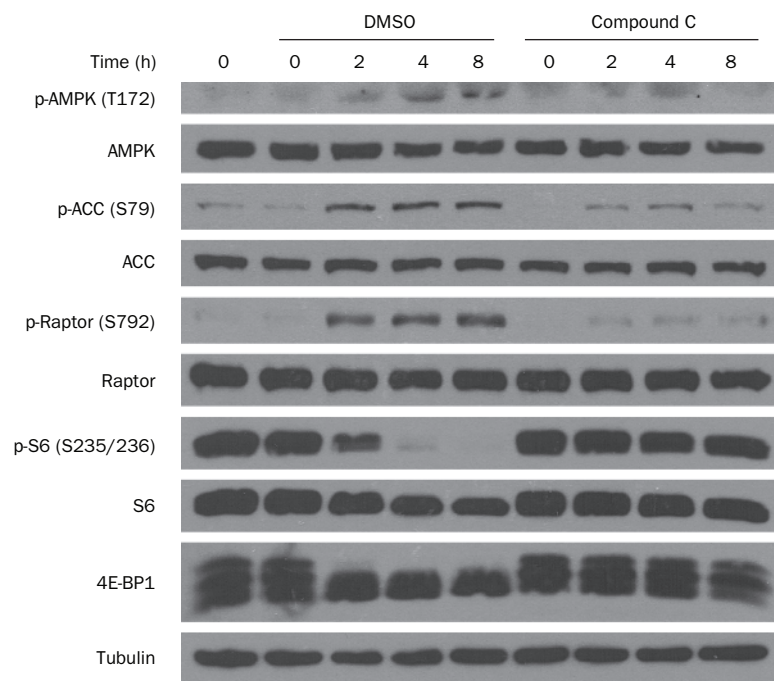


Figure 7 | Western blot of UOK262 cells treated with 1 mM 2DG for the indicated periods of time in the presence of compound C (an AMPK inhibitor) or DMSO (vehicle). Treatment with 1 mM 2DG results in the activation of AMPK, determined here by increased phosphorylation of the α subunit and of its substrates ACC and Raptor, which is observed at 2 h and persists throughout the experiment. AMPK activation correlates with the inhibition of mTORC1, shown by a reduction in the level of phospho-S6 and, more directly, by decreased phosphorylation of the mTORC1 substrate 4E-BP1 (shown here by disappearance of the highly phosphorylated slow migrating form at the top). AMPK has been previously shown to inactivate mTORC1.²⁹ To determine whether the inhibition of mTORC1 was mediated by AMPK, we tested whether mTORC1 inhibition by 2DG could be blocked by treatment with a drug preventing the activation of AMPK. As shown in the right panel, compound C, an AMPK inhibitor, markedly blunted AMPK activation by 2DG, which blocked mTORC1 inactivation. Abbreviations: 2DG, 2-deoxy-D-glucose; 4E-BP1, initiation factor 4E-binding protein 1; ACC, acetyl-CoA carboxylase; AMPK, AMP-activated protein kinase; DMSO, dimethyl sulfoxide; mTORC1, mammalian target of rapamycin complex 1; Raptor, regulatory-associated protein of mTOR.

Treatment and management

As illustrated by poly(ADP-ribose) polymerase (PARP) inhibitors in *BRCA1/2*-deficient tumors,²⁴ the loss of particular gene functions in tumors may create a state of dependency on specific pathways that, when disrupted therapeutically, may result in selective tumor killing. The *BRCA1/2* proteins are required for DNA repair by homologous recombination, and inactivation of this pathway renders cells dependent on nonhomologous DNA repair mechanisms, which, when inhibited, cause selective tumor cell death.²⁵

RCC offers a unique opportunity for molecular-based therapeutic approaches,²⁶ and we reasoned that the *FH* enzymatic deficiency in the tumor, with consequent truncation of the TCA cycle, should render tumor cells dependent on glycolysis for ATP generation. This hypothesis was supported by evidence from several laboratories showing that *FH*-deficient cells accumulate TCA cycle intermediates and do not grow on nonfermentable carbon sources.^{12,18,19} Furthermore, an *FH*-deficient

cell line (UOK262) that was generated from a pRCC-2 metastasis in a patient with HLRCC was shown to have profoundly impaired mitochondrial respiration, which is linked to the TCA cycle, and to be exquisitely dependent on glucose for cell proliferation and survival.¹¹ Given the indispensable nature of ATP for basic cellular processes, such as the generation and maintenance of a membrane potential and protein translation, disruption of glycolysis and ATP production in tumor cells would be expected to result in their demise.

As continuous 2DG blocked the proliferation of *FH*-deficient cells *in vitro*, we sought to further characterize the effects of 2DG in this setting (Box 3, Figures 6,7). Our results showed that, at pharmacologically relevant concentrations, 2DG activates AMP-activated protein kinase (AMPK) in *FH*-deficient cells, leading to AMPK-mediated inhibition of mTORC1. Given the importance of mTORC1 for cell growth and proliferation, mTORC1 inhibition may contribute to the antiproliferative effects of 2DG. The current patient had been previously treated with an mTORC1 inhibitor, to which the tumor had become resistant; thus, the tumor would have been expected to be similarly resistant to mTORC1 inhibition mediated by 2DG.

Conclusions

In this Case Study, we describe a patient with *FH*-deficient pRCC-2 treated with 2DG. To our knowledge, this is the first report exploring glycolytic inhibitors in tumors deficient for a TCA cycle enzyme.

A novel germline *FH* mutation was identified. While DNA testing of the patient's parents was not performed, the absence of HLRCC symptoms in the parents suggests that the mutation occurred *de novo*. The type of mutation (nonconservative missense mutation of a universally conserved residue), combined with the results of structural studies, reconstitution experiments and functional studies in the tumor, strongly suggested that this was a loss-of-function mutation. Together with the finding of LOH in the tumor and the clinical presentation, these data established the diagnosis of HLRCC.

We reasoned that *FH* deficiency in the tumor would result in a vulnerability that could be exploited therapeutically for the benefit of the patient. Most tumors are thought to primarily utilize glycolysis for ATP generation, a phenomenon known as the Warburg effect.²⁷ Because of the inefficient ATP generation by glycolysis, these tumors are glucose avid, which is the foundation for ¹⁸F-FDG-PET imaging.²⁸ This dependency on glycolysis would be expected to be further exacerbated by mutations disrupting the TCA cycle. Thus, tumors such as the one in the patient described here represent a unique opportunity for the evaluation of glycolytic inhibitors, which are being considered as broad anticancer agents.²⁰ Despite a compelling foundation upon which to evaluate 2DG in our patient, the treatment was ultimately unsuccessful. Our *in vitro* modeling of once-daily 2DG dosing suggested that this regimen was insufficient to abrogate tumor cell proliferation. By contrast, sustained 2DG exposure blocked cell proliferation. However,

more-frequent administration of 2DG in the patient did not result in obvious antitumor activity, at least as determined by ^{18}F FDG-PET/CT. Although the treatment duration was short, if ATP generation had been effectively blocked in the tumor, we would have expected to see an effect even in this small window of time.

Our data show that, at pharmacologically achievable concentrations, 2DG activated AMPK, resulting in AMPK-dependent inhibition of mTORC1 in *FH*-deficient cells. It remains to be determined whether 2DG similarly inactivates mTORC1 in tumors *in vivo*. *In vitro* studies showed that 2DG did not substantially affect glycolysis or ATP levels at pharmacologically

relevant concentrations; however, continuous 2DG administration in the patient did result in symptoms of hypoglycemia indicative of successful glycolysis inhibition. The development of hypoglycemic symptoms, together with the lack of antitumor effect, suggests that even in tumors that may be particularly addicted to glycolysis, the therapeutic window may be narrow, if existent at all. However, whether hypoglycemic symptoms were exacerbated by the heterozygous *FH* state of the current patient is unknown. Thus, further investigations are needed to determine whether therapeutic strategies that aim to disrupt glycolysis in tumors will be feasible and effective.

- Hudes, G. *et al.* Temsirolimus, interferon alfa, or both for advanced renal-cell carcinoma. *N. Engl. J. Med.* **356**, 2271–2281 (2007).
- Motzer, R. J. *et al.* Efficacy of everolimus in advanced renal cell carcinoma: a double-blind, randomised, placebo-controlled phase III trial. *Lancet* **372**, 449–456 (2008).
- Tomlinson, I. P. *et al.* Germline mutations in *FH* predispose to dominantly inherited uterine fibroids, skin leiomyomata and papillary renal cell cancer. *Nat. Genet.* **30**, 406–410 (2002).
- Toro, J. R. *et al.* Mutations in the fumarate hydratase gene cause hereditary leiomyomatosis and renal cell cancer in families in North America. *Am. J. Hum. Genet.* **73**, 95–106 (2003).
- Gottlieb, E. & Tomlinson, I. P. Mitochondrial tumour suppressors: a genetic and biochemical update. *Nat. Rev. Cancer* **5**, 857–866 (2005).
- Lehtonen, H. J. *et al.* Increased risk of cancer in patients with fumarate hydratase germline mutation. *J. Med. Genet.* **43**, 523–526 (2006).
- Grubb, R. L. 3rd *et al.* Hereditary leiomyomatosis and renal cell cancer: a syndrome associated with an aggressive form of inherited renal cancer. *J. Urol.* **177**, 2074–2079 (2007).
- Bayley, J. P., Launonen, V. & Tomlinson, I. P. The *FH* mutation database: an online database of fumarate hydratase mutations involved in the MCUL (HLRCC) tumor syndrome and congenital fumarase deficiency. *BMC Med. Genet.* **9**, 20 (2008).
- Weaver, T. M., Levitt, D. G., Donnelly, M. I., Stevens, P. P. & Banaszak, L. J. The multisubunit active site of fumarase C from *Escherichia coli*. *Nat. Struct. Biol.* **2**, 654–662 (1995).
- Isaacs, J. S. *et al.* HIF overexpression correlates with biallelic loss of fumarate hydratase in renal cancer: novel role of fumarate in regulation of HIF stability. *Cancer Cell* **8**, 143–153 (2005).
- Yang, Y. *et al.* UOK 262 cell line, fumarate hydratase deficient (*FH*⁻/*FH*⁺) hereditary leiomyomatosis renal cell carcinoma: *in vitro* and *in vivo* model of an aberrant energy metabolic pathway in human cancer. *Cancer Genet. Cytogenet.* **196**, 45–55 (2010).
- O'Flaherty, L. *et al.* Dysregulation of hypoxia pathways in fumarate hydratase-deficient cells is independent of defective mitochondrial metabolism. *Hum. Mol. Genet.* **19**, 3844–3851 (2010).
- Kiuru, M. *et al.* Few *FH* mutations in sporadic counterparts of tumor types observed in hereditary leiomyomatosis and renal cell cancer families. *Cancer Res.* **62**, 4554–4557 (2002).
- Morris, M. R. *et al.* Molecular genetic analysis of *FH*-1, *FH*, and *SDHB* candidate tumour suppressor genes in renal cell carcinoma. *J. Clin. Pathol.* **57**, 706–711 (2004).
- Sudarshan, S., Pinto, P. A., Neckers, L. & Linehan, W. M. Mechanisms of disease: hereditary leiomyomatosis and renal cell cancer—a distinct form of hereditary kidney cancer. *Nat. Clin. Pract. Urol.* **4**, 104–110 (2007).
- Choueiri, T. K. *et al.* Efficacy of sunitinib and sorafenib in metastatic papillary and chromophobe renal cell carcinoma. *J. Clin. Oncol.* **26**, 127–131 (2008).
- Plimack, E. R. *et al.* Sunitinib in papillary renal cell carcinoma (pRCC): results from a single-arm phase II study. *J. Clin. Oncol.* **28**, 4604 (2010).
- Pollard, P. J. *et al.* Accumulation of Krebs cycle intermediates and over-expression of HIF1 α in tumours which result from germline *FH* and *SDH* mutations. *Hum. Mol. Genet.* **14**, 2231–2239 (2005).
- Sudarshan, S. *et al.* Fumarate hydratase deficiency in renal cancer induces glycolytic addiction and hypoxia-inducible transcription factor 1 α stabilization by glucose-dependent generation of reactive oxygen species. *Mol. Cell Biol.* **29**, 4080–4090 (2009).
- Pelicano, H., Martin, D. S., Xu, R. H. & Huang, P. Glycolysis inhibition for anticancer treatment. *Oncogene* **25**, 4633–4646 (2006).
- Stein, M. *et al.* Targeting tumor metabolism with 2-deoxyglucose in patients with castrate-resistant prostate cancer and advanced malignancies. *Prostate* **70**, 1388–1394 (2010).
- Raez, L. E. *et al.* Responses to the combination of the glycolytic inhibitor 2-deoxy-glucose (2DG) and docetaxel (DC) in patients with lung and head and neck (H/N) carcinomas. *J. Clin. Oncol.* **25**, 14025 (2007).
- Alam, N. A. *et al.* Genetic and functional analyses of *FH* mutations in multiple cutaneous and uterine leiomyomatosis, hereditary leiomyomatosis and renal cancer, and fumarate hydratase deficiency. *Hum. Mol. Genet.* **12**, 1241–1252 (2003).
- Fong, P. C. *et al.* Inhibition of poly(ADP-ribose) polymerase in tumors from *BRCA* mutation carriers. *N. Engl. J. Med.* **361**, 123–134 (2009).
- Farmer, H. *et al.* Targeting the DNA repair defect in *BRCA* mutant cells as a therapeutic strategy. *Nature* **434**, 917–921 (2005).
- Linehan, W. M. *et al.* Hereditary kidney cancer: unique opportunity for disease-based therapy. *Cancer* **115**, 2252–2261 (2009).
- Vander Heiden, M. G., Cantley, L. C. & Thompson, C. B. Understanding the Warburg effect: the metabolic requirements of cell proliferation. *Science* **324**, 1029–1033 (2009).
- Mankoff, D. A. *et al.* Tumor-specific positron emission tomography imaging in patients: [^{18}F] fluorodeoxyglucose and beyond. *Clin. Cancer Res.* **13**, 3460–3469 (2007).
- Inoki, K., Zhu, T. & Guan, K. L. TSC2 mediates cellular energy response to control cell growth and survival. *Cell* **115**, 577–590 (2003).
- Kimura, N. *et al.* A possible linkage between AMP-activated protein kinase (AMPK) and mammalian target of rapamycin (mTOR) signalling pathway. *Genes Cells* **8**, 65–79 (2003).

Acknowledgments

This manuscript is dedicated to the memory of the patient and to her family whose request it was that the findings be reported so that others may potentially benefit. pBabe-FH-flag was a gift from Dr Sunil Sudarshan (University of Texas Health Science Center, San Antonio, TX) and UOK262 cells were a gift from Dr Youfeng Yang and Dr W. Marston Linehan (National Cancer Institute, Bethesda, MD). We are grateful to Dr Samuel Peña-Llopis, Sharanya Sivanand and Jessica Gillen for tissue collection and processing, Dr Virginia Langmuir and Stew Kroll at Threshold Pharmaceuticals for providing the drug and for advice, Capt. Frank H. Cross Jr at the FDA, the Simmons Cancer Center pharmacy and nursing staff, and the Brugarolas lab. T. A. T. Tran was supported by a T32CA124334 grant, and R. J. DeBerardinis was supported by NIH (DK072565) and CPRIT (HIRP100437) grants. This research was supported by the following grants to J. Brugarolas: Clinical Scientist Development Award from the Doris Duke Charitable Foundation (2007062), K08NS051843, R01CA129387 and CPRIT (RP101075). J. Brugarolas is a Virginia Murchison Linthicum Scholar in Medical Research at UT Southwestern.

Author contributions

T. Yamasaki designed and carried out most experiments. T. A. T. Tran was responsible for the site-directed mutagenesis and the native gel electrophoresis. O. K. Oz evaluated the PET scans, X. Zhang performed the crystallographic analyses, and R. J. DeBerardinis was involved in discussions. G. V. Raj and R. E. Schwarz contributed to the care of the patient and were responsible for the initial and subsequent surgeries, respectively. J. Brugarolas was the patient's primary oncologist, directed the project, and wrote the manuscript. T. Yamasaki and all the authors reviewed and made suggestions to the manuscript.

Supplementary information

Supplementary information is linked to the online version of the paper at www.nature.com/nrurlo.